EFFECT OF FRACTURE SURFACE FRACTAL DIMENSION ON HYDROGEN CONCENTRATION OF STAINLESS STEELS

FENG Jie, TAN Yun, TAO Ping, FAN Ying

Institute of Systems Engineering, China

Properties of hydrogen embrittlement of 1Cr18Ni9Ti and 21-6-9 stainless steels were investigated by hydrogen atmosphere thermal charging. At the same time, the fracture fractal dimensions of samples in different hydrogen-charging time were measured using the Vertical Section Method. The relationship of fractal dimension and the properties of hydrogen embrittlement were analyzed. The results shown that the hydrogen content of samples and the loss of plastic properties increased along with the time of hydrogen charging, but the reduction of area decreased. For the fracture morphology, the fractal dimension decreased with the time of hydrogen charging. Good corresponding linear relationship existed between the fractal dimension and the reduction of area. The fractal dimension could reflect the effects of hydrogen to the materials.

Introduction

Metal fracture surface quantitative analysis became importance of material deformation and rupture investigation recently. It could supply another supplementary information for the metallurgical phase method. Coster[1] had a nice review about the headway for this line, and fractal characterization of fracture surface was regarded as one of comparatively innovative way. It was a type of scale for metal fracture surface roughness.

The mechanical properties of materials were related to the fracture mechanism directly, especially during microscopic fracture events and crack extending process. Therefore, quantitative fractography played an important role in material research by using both optical microscope and scanning electron microscope (SEM). In 1984, Mandelbrot [2] first introduced the concept of fractal dimension to materials science in order to discover the affiliation between mechanical properties and the tortuosity of fracture surfaces, consequently, fractal was used to describe such self-affine nature of the body with irregular geometrical shape. Many methods [3–6] were invented to measure the fractal dimension of fracture surface, among which *slit island method* and *vertical sectioning method* were the most effective ones. Although some contradiction was found between those two methods, most researchers chose the vertical sectioning method since it related better with the properties. In recent studies [7–11], this analysis method had achieved great results in theoretic simulation as well as in solving practical problems.

In the study of interaction of metal material and hydrogen, due to hydrogen embrittlement, material turned to brittle rupture translating, on the fracture it was reflected by material transiting from ductile fracture surface to rock-candy structure.

Due to austenitic stainless steels took on favorable anti-hydrogen performance, generally it was ductile rupture. But characteristic of brittle rupture were became conscious on the old research [10~12]. In order to quantitatively describing trend of material occurring brittle rupture, the concept of fractal was introduced for fracture analyses, which could strike up relation of material hydrogen content, performance and fractal dimension. The fractal study also supplied the gist for analyses fracture pattern of material and estimation material hydrogen embrittlement degree.

The purpose of the paper was researching fractal dimension of fracture surface for different metal tensile sample at different thermal-hydrogen-charging condition, founding empirical relation between material hydrogen content and mechanical properties and fractal dimension. From analyses fracture fractal dimension, material hydrogen embrittlement degree could be estimated. It is hoped that a new type of criteria of material hydrogen-embrittlement could be obtained.

1. Materials and testing methods

1.1. Testing materials and specimens

The materials of this research were two type of alloy, 1Cr18Ni9Ti (shortened form 18-8) and 21-6-9 stainless steels. The chemical compositions of the testing alloys were shown in Tab. 1.

Table 1

The chemical compositions of the testing alloys

Alloys	Chemical compositions (wt%)						
	Cr	Ni	Mo	Ti	Mn	Si	C,S,P
18-8	18,2	9,6	/	0,42	1,48	0,47	trace
21-6-9	20,2	7,2	0,23	/	9,4	0,48	

Specimens were cut from a claviform steel of diameter 20mm and machined to tensile samples of diameter 5mm and nominal length 25mm.

1.2. Thermal-hydrogen-charging test and mechanical test

The alloys were saturated with hydrogen by using the thermal-hydrogen-charging. This process was undergone with high-pressure gaseous hydrogen charging device designed by ourselves. After being cleaned, the specimen were put into this device to charge hydrogen, the charging conditions were 200 °C, 24 MPa, 99,999 % H_2, and the hydrogen-charging times were respectively, 0 hour (no hydrogen charging), 24 hours, 60 hours, 120 hours, 240 hours. After hydrogen-charging, the hydrogen concentration of specimens was measured by type QCY-2 apparatus (analytic precision is 0,1 ppm).

Tensile testing was engaged on MTS 810 material test system. The velocity of testing was 0,5 mm/min, and the velocity of strain was $3{,}3\times10^{-4}$/s. The anti-hydrogen-embrittlement performance was analyzed according to the test result. Defining anti-hydrogen-embrittlement index I_ψ is:

$$I_\psi = (\psi - \psi_H)/\psi \times 100\ \%. \quad (1)$$

Where ψ is the percent reduction of area of origin specimen, ψ_H is the percent reduction of area of specimen after thermal-hydrogen-charging.

ψ_H is bigger more and I_ψ smaller more, the anti-hydrogen-embrittlement performance of materials is nice more.

1.3. Measure method of the fractal dimension of the fracture surface

The Vertical Section Method was applied and an improvement was made to calculate the fractal dimensions of the morphology of fractures. At cross-sectional view of perpendicular fracture surface, the fracture surface was presented a slip of anomalous curve. The length of irregularity plane curve was a function of the measure yardstick, it is:

$$\lg L(\eta) = \lg L_0 - (D-1)\lg\eta. \quad (2)$$

Where L_0 is constant with length dimensional, D is the fractal dimension of the curve.

The slope of straight line α was fitting out using linear regression method of lgη and $\lg L(\eta)$, Then:

$$D - 1 = \alpha. \quad (3)$$

Toward tensile sample fracture, two section plane of decussating on perpendicular fracture direction by metallographic polishing were chosen and were magnified up to 1000 times. Length of the curve of cross-sectional view were measured with differ yardstick. The least yardstick is 1mm and it was correspond to 1 micron. Through the formula we could get the fracture curvilinear fractal dimension D.

According to Zero-sets, the fractal dimension Ds of the fractured surface was:

$$Ds = 1 + D. \quad (4)$$

2. Results and discussion

2.1. Tensile properties

The results of tensile test and anti-hydrogen-embrittlement test were shown in Tab. 2. The relation curve of tensile properties and hydrogen contents of samples with hydrogen-charging time were shown in Fig. 1~Fig. 4.

Table 2

The test results of tensile properities and anti-hydrogen-embrittlement

Alloy	Time of hydrogen-charging (h)	hydrogen consistence (ppm)	$\sigma_{0,2}$, (MPa)	σ_b. (MPa)	δ_5, (%)	φ, (%)	I_φ, (%)
18-8	0	5,1	580,2	812,4	47,3	68,0	0
	24	18,8	573,2	802,1	40,1	49,8	26,8
	60	25,0	56,3	783,0	30,1	37,0	45,6
	120	31,2	608,6	813,5	34,3	36,1	46,9
	240	40,7	610,6	833,7	41,0	32,1	52,8
21-6-9	0	1,6	435,6	786,0	63,1	77,8	0
	24	23,8	430,8	790,7	60,0	66,0	15,2
	60	34,5	450,7	788,3	57,7	67,5	13,2
	120	44,9	468,9	799,3	63,9	62,1	20,2
	240	59,5	471,7	807,5	57,9	59,5	23,5

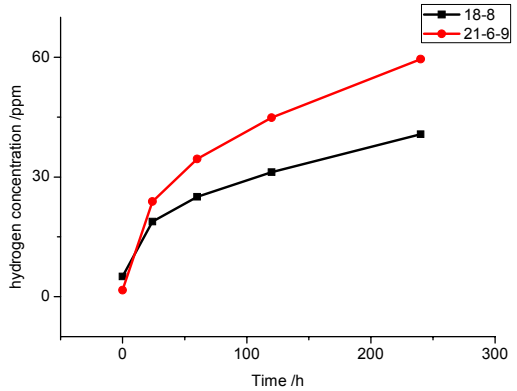

Fig. 1. Curve of hydrogen concentration and time of hydrogen-charging

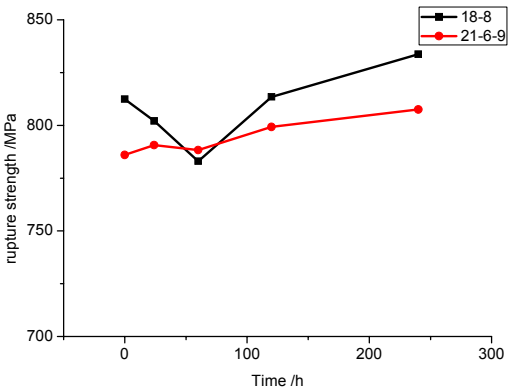

Fig. 2. Curve of σ_b and time of hydrogen-charging

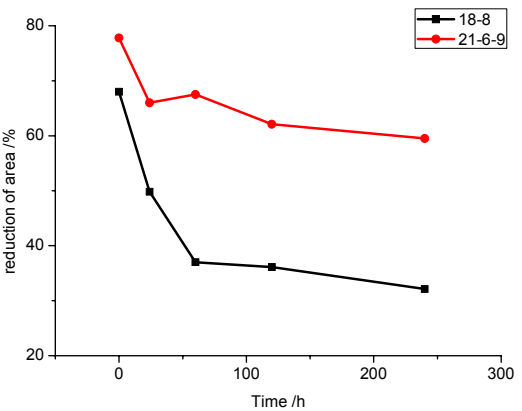

Fig. 3. Curve of ψ and time of hydrogen-charging

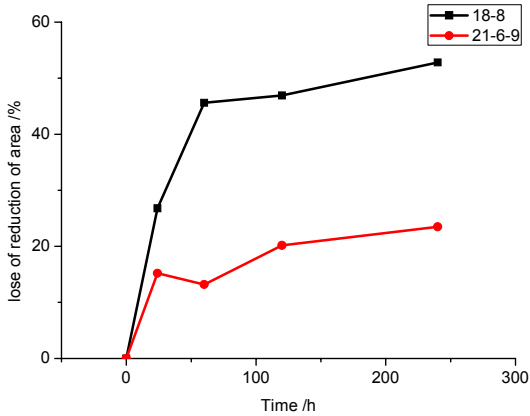

Fig. 4. Curve of $I\psi$ and time of hydrogen-charging

2.1.1. Material interior hydrogen concentration was step up with the time of hydrogen-charging increasing. For the two kinds of materials, hydrogen interior concentration were very different in the same conditions of hydrogen-charging. It was mostly related with material internal structure and hydrogenous solubility. It can not totally reflect material sensitivity to hydrogen.

2.1.2. The strength of material was not evidently influenced by the hydrogen-charging. Along with the increase of the interior hydrogen concentration the strength of material was a little increased for normal austenitic stainless steel 18-8 and 21-9-6. Due to their face-centered cubic structure of the crystal, the dissolved hydrogen in material should gradually occupy austenitic octahedral interstices position and each vice location. It was the work of solution strength for material and bring about increase of its strength.

2.1.3. These were not distinguished influence by hydrogen for material extensibility. So the influence of hydrogen to material could not be judged with extensibility of tensile sample of material.

2.1.4. The reduction of area ψ and the anti-hydrogen-embrittlement index I_ψ were changed along with hydrogen-charging time extending. With the increasing of interior hydrogen concentration of material, the reduction of area ψ decreased, but the anti-hydrogen-embrittlement index I_ψ increased. The two kinds of materials were indicatively different, which reflected the difference of anti-hydrogen performance of the two materials. It was said that 21-6-9 has better anti-hydrogen-embrittlement performance than 18-8 less.

2.2. Fractal dimension of fracture morphology

The fractal dimension of material was measured by adopting *vertical sectioning method*.

10 different sections perpendicular to fracture were selected for each set of samples, the length of a curve of cross-sectional view for each section were measured with different yardstick by image analysis instrument. The results were drawn

up at logarithmic coordinates and the slope coefficient was fitted out. Fractal dimension of each cross-sectional could be solved according to the formulae.

Fracture fractal dimension of each material were shown in Tab. 3. The curve of thermal-hydrogen -charging time and fracture fractal dimension were shown in Fig. 5. It was shown that the fractal dimension was reduced with material plasticity decreasing due to the hydrogen. The variance trend was conformable with reduction of area.

The relationship of fracture fractal dimension and material reduction of area was researched. The relationship of the fractal dimension with reduction of area of two kinds of materials was shown clearly in the fig.6. It was observed from the picture that the decrease scale of fractal dimension submit approximately linear relationship with the reduction of area. That was said that the material hydrogen embrittlement degree could be estimation through material fracture fractal dimension.

Like the definition of hydrogen reduction of area decrease $I\psi$, we could define the fractal dimension decrease I_D. It was:

$$I_D = 1-(Ds_H - 2)/(Ds - 2). \quad (5)$$

In the formula, D_{SH} was the fractal dimension of hydrogen-charging, Ds was the fractal dimension of no hydrogen-charging.

Through the I_D variation we could estimation the change state of material plastic, and could also estimation the degree of hydrogen-embrittlement of material.

Because the fractal dimension was reflection of fracture roughness, the influence of hydrogen to fracture fractal dimension could be reflected qualitatively on the fracture pattern of tensile sample.

The SEM image of fracture of two kinds of material were shown in fig. 7~ fig. 8. It was shown that the fracture of sample of no charged hydrogen were all the dimples type ductile rupture for two kinds of material. The dimple was getting gradually shallower, at the same time, appeared a spot of level area and fracture presented dimple and quasi cleavage fracture mixed image when material interior hydrogen concentration increased. Especially for 18-8 steel, cleavage fracture pattern showed rock candy like features at thermal-hydrogen-charging of 240h. It was said that the material hydrogen embrittlement degree was serious. The variation trend was coincidence of the measurement result of fracture fractal dimension.

In brief, it was observed from the fractal analyses and material property that interior hydrogen concentration was increased and the influence of hydrogen to material plastic tend towards serious along with increase of thermal-hydrogen-charging time. Its reflection on material property was that the reduction of area decrease and reduction of area of material was larger. Hydrogen influence reflected in material fracture image was mostly behaved as material fracture pattern from dimple rupture turn into dimple and quasi cleavage mixed type fracture pattern. We could quantitatively describe the influence of hydrogen to material property through measure fracture fractal dimension. That was said that the fracture fractal dimension was decreased with the material interior hydrogen concentration increase. Fracture was from intricacy to simplicity with the loss of fracture fractal dimension increase. It was obvious that it could quantitatively describe the influence of hydrogen to material property through measure of fracture fractal dimension.

Table 3

Results of fracture fractal dimension

Alloys	charging time (h)	D	R_D	Ds	I_D(%)
18-8	0	1,1731	0,0088	2,173	0
	24	1,1382	0,0067	2,138	20,2
	60	1,1285	0,0068	2,128	26,0
	120	1,0883	0,0039	2,088	49,1
	240	1,0893	0,0048	2,089	48,6
21-6-9	0	1,1888	0,0040	2,189	0
	24	1,1508	0,0076	2,151	20,1
	60	1,1553	0,0092	2,155	18,0
	120	1,1192	0,0079	2,119	37,0
	240	1,1211	0,0039	2,121	36,0

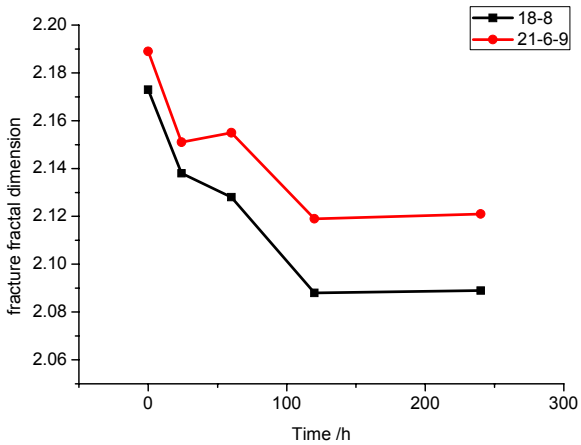

Fig. 5. Curve of fracture fractal dimension and time of hydrogen charging

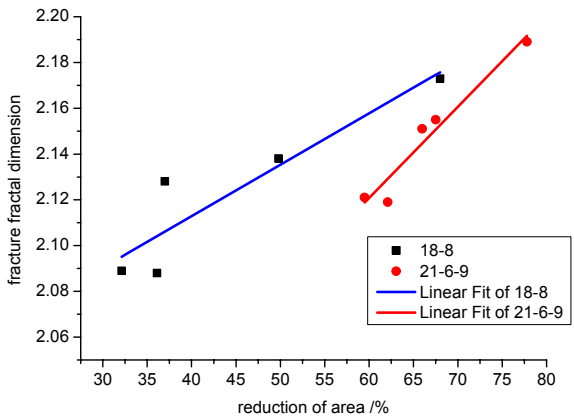

Fig. 6. Curve of loss of fracture fractal dimension and reduction of area

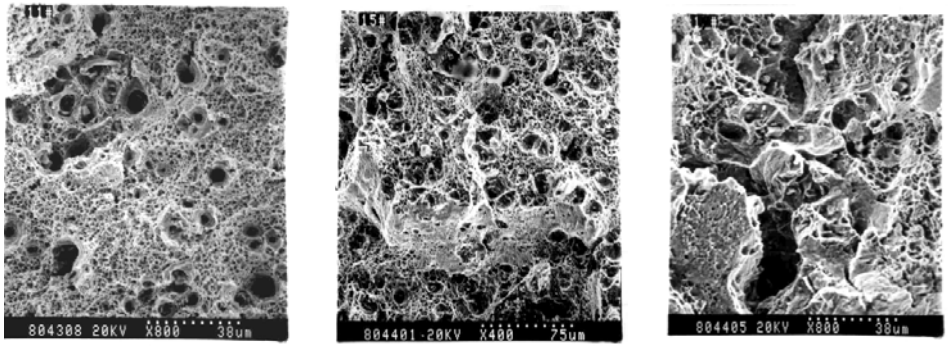

a) no hydrogen-charging b) 60 h of hydrogen-charging c) 240h of hydrogen-charging

Fig. 7. Rupture SEM of 18-8 steel

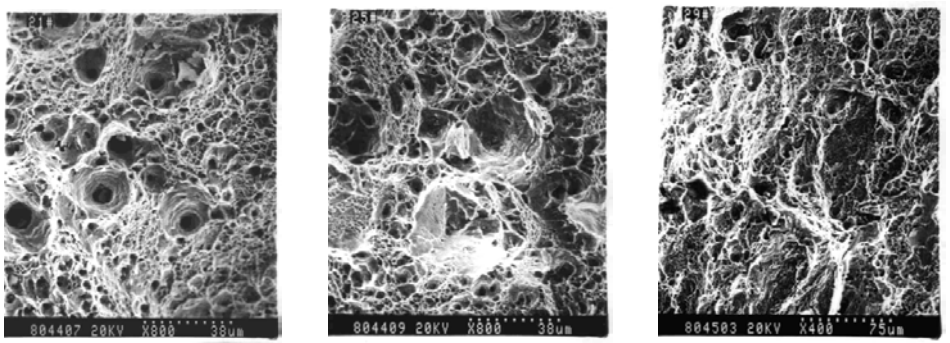

a) no hydrogen-charging b) 60 h of hydrogen-charging c) 240h of hydrogen-charging

Fig. 8. Rupture SEM of 21-6-9 steel

3. Conclusion

3.1. With increase of the hydrogen-charging-time, the hydrogen concentration of 18-8 and 21-6-9 steels were increased and the reduction of area also decreased. The fracture fractal dimension of the materials submitted decrease trend. The fracture fractal dimension and reduction of area of two kinds of material submitted approximation linear relationship.

3.2. Through comparing reduced degree for reduction of area, we could estimate material susceptible degree to hydrogen and anti-hydrogen embrittlement behaviors. At the same time, we could decide the material anti-hydrogen behavioral through comparison loss of fractal dimension degree. The results were accordant: The anti-hydrogen-embrittlement performance of 18-8 steel was less and the anti-hydrogen-embrittlement performance of 21-6-9 steel was good.

3.3. Along with the hydrogen-charging-time and the hydrogen concentration of material increase, material fracture pattern reflected qualitative to: dimples of fracture becoming from large and deep to fleet and flat, part region fracture morphology appeared the quasi cleavage or cleavage fracture. It was shown that fracture

morphology changed from coarseness to smoothness, and the fracture fractal dimension was diminished. Fracture fractal dimension could ration descript fracture image.

3.4. The fractal dimension might be used to characterize the influence of hydrogen to materials properties in quantity. It was said that fracture fractal dimension could judge susceptible the degree of hydrogen to material. The method of the fractal dimension could become a sort of new way to research properties influencing of hydrogen to materials.

Acknowledgments

This work was supported by the project of foundation technology No. Z112012B001.

References

1. Coster M., Chermant J. L. Int Metall Rev, 1983; 28:328.

2. Manderlbrot B. B., Passoja D. E., Paullay A. J. Nature, 1984; 308:721.

3. Lung C. W., Pietronero L., Tosatti E. eds. Fractals in Physics, Elsevier Science Publishers B V, 1986: 189.

4. Pande C. S., Richards L. E., Louat N., Dempsey B. D., Schwoeble A. J. Acta Metall, 1987: 35:1633.

5. Pilling J., Ridley N. Res Mech, 1988; 23: 31.

6. Lung C. W., Mu Z. Q. Phys Rev, B, 1988; 38: 11781.

7. Kamila Amato de Campos, Celso Yoshino, Luis Rogerio de Oliveira Hein, Materials Science and Engineering A, 525 (2009) 37–41.

8. Wei Tanga, YongWanga, Applied Surface Science, 258 (2012) 4777–4781.

9. Myung Chang Kanga, Jeong Suk Kima, Kwang Ho Kim, Surface & Coatings Technology 193 (2005) 259– 265.

10. Long Qiyi, Wen Youhai, Zhu Zumin, et al. Transactions of Metal Heat Treatment, V15(1994): 19-25.

11. WANG Liang, WANG Li-dong, FEI Wei-dong. Trans. Nonferrous Met. Soc. China 21(2011): 461-466.

12. Li Xiuyan, Li Yiyi, *Hydrogen Damaged of Austenitic Alloy*, Beijin, Sci. Pess., 2003.